JOURNAL OF GUIDANCE, CONTROL, AND DYNAMICS
Vol. 27, No. 4, July–August 2004

Dynamic Optimization Strategies for Three-Dimensional Conflict Resolution of Multiple Aircraft

Arvind U. Raghunathan*
Carnegie Mellon University, Pittsburgh, Pennsylvania 15213
Vipin Gopal†
United Technologies Research Center, East Hartford, Connecticut 06108
Dharmashankar Subramanian‡
Honeywell International, Minneapolis, Minnesota 55418
Lorenz T. Biegler§
Carnegie Mellon University, Pittsburgh, Pennsylvania 15213
and
Tariq Samad¶
Honeywell International, Minneapolis, Minnesota 55418

Free flight is an emerging paradigm in air traffic management. Conflict detection and resolution is the heart of any free-flight concept. The problem of optimal cooperative three-dimensional conflict resolution involving multiple aircraft is addressed by the rigorous numerical trajectory optimization methods. The conflict problem is posed as an optimal control problem of finding trajectories that minimize a certain objective function while the safe separation between each aircraft pair is maintained. The initial and final positions of the aircraft are known and aircraft models with detailed nonlinear point-mass dynamics are considered. The protection zone around the aircraft is modeled to be cylindrical in shape. A novel formulation of the cylindrical protection zone is proposed by the use of continuous variables. The optimal control problem is converted to a finite dimensional nonlinear program (NLP) by the use of collocation on finite elements. The NLP is solved by the use of an interior point algorithm that incorporates a novel line search method. A reliable initialization strategy that yields a feasible solution on simple models is also proposed and adapted to detailed models. Several resolution scenarios are illustrated. The practical issue of flyability of the generated trajectories is addressed by the ability of our mathematical programming framework to accommodate detailed dynamic models.

I. Introduction

AIR traffic control (ATC) systems require a vast network of people and equipment to ensure the safe operation of commercial aircraft. The air traffic controllers coordinate the movements of the aircraft to make certain that they are separated by a minimum distance. The immediate concern is safety, but controllers also must direct planes efficiently to minimize delays. The current ATC system prescribes predefined routes and flight procedures for all aircraft to ensure sufficient separation among them. In this infrastructure, the lateral separations are guaranteed by different choice of flight routes and the vertical separation by different flight levels, and longitudinal separations are maintained through speed changes. Today's practices often result in planes moving from point to point along corridors, resulting in lost time and fuel and, hence, lost revenues.

Recently, the aviation community has put forth a concept called free flight[1] that will serve as the operating paradigm for future ATC. The change will require new concepts of shared responsibility between controllers and aircraft operators. Currently, controllers assign routes, altitudes, and speeds. Under the new system, aircraft operators can change them in real time. Controllers would only intervene to ensure that aircraft remain at safe distances from one another. Air traffic controllers will be central to ensuring safety, but will eventually shift from controlling to monitoring flights. The free-flight environment will also enable the minimization of individual aircraft operating costs. The key to the success of the free-flight concept is the detection of conflicts and determination of appropriate strategies for the resolution of conflict among aircraft. Our work focuses on resolving conflicts among aircraft in a manner that is optimal to the participating aircraft.

Current ATC standards specify the minimum separation between any two aircraft. If two aircraft are at the same flight level, the geometrical distance between them must be larger than 5 n mile. If the two aircraft are roughly in the same horizontal position, their vertical separation must be larger than or equal to 2000 ft. The horizontal separation distance requirement reduces to 3 n mile when aircraft are within 40 n mile from radar antennas, and the vertical separation requirement becomes 1000 ft for aircraft below 29,000 ft. Two aircraft are termed to be in conflict if one aircraft encroaches into the protected zone of the other.

Several studies have previously looked at resolution of conflicts between aircraft in free flight. Hwang and Tomlin[2] propose a protocol-based conflict resolution method for multiple aircraft in ATC. They derive protocol for three-aircraft conflict resolutions; however, their methods are general and can be extended to the N-aircraft case. The aircraft are assumed to be at the same altitude, and conflicts are resolved in the horizontal plane by the use of heading change. In this case, the protected zone around each aircraft reduces to a circular envelope. Zhao and Schultz[3] have examined conflict resolution problems of two aircraft described by the same dynamics as given earlier. The conflict-free trajectories are obtained as solutions of an optimal control problem that minimizes

Received 10 September 2002; revision received 15 January 2004; accepted for publication 27 January 2004.

*Graduate Student, Department of Chemical Engineering.
†Group Leader, Dynamic Modeling and Analysis.
‡Research Scientist, Honeywell Automation and Control Solutions.
§Professor, Department of Chemical Engineering.
¶Corporate Fellow, Honeywell Automation and Control Solutions.

deviations from intended flight paths. Terminal constraints are included to force each aircraft to return to its original path. They also discuss extensions for the case of multiple aircraft. Frazzoli et al.[4] consider resolution of conflicts among aircraft using semidefinite programming. Hu et al.[5] study the problem of finding the optimal three-dimensional conflict-free maneuvers for multiple aircraft. The candidate maneuvers include changes of altitude, heading, and speed. Among all conflict-free maneuvers, they choose one that minimizes a certain energy function. They propose a geometrical construction and a numerical algorithm to determine the optimal maneuver for the two-aircraft case. As for the multi-aircraft case, an approximation scheme is used to compute a suboptimal two-legged solution. The effectiveness of the approach is illustrated by a number of examples. Three-dimensional trajectory optimization algorithms have been employed by Menon et al.[6] to obtain conflict free-flight paths. The algorithms use nonlinear point-mass models and include realistic operational constraints on individual aircraft. The protected zone of aircraft are modeled as an ellipsoid that superscribes the cylindrical protected zone. The resulting problem is nonconvex. In addition, the ellipsoidal constraints do not provide a tight representation of the feasible region. The resulting solutions may be improved, however, when the protection zone is modeled as a cylinder. In this work, we eliminate this drawback by modeling the protection zone directly as cylinders.

In addition, we study cooperative conflict resolution of aircraft described by nonlinear point-mass models. This paper builds on previous work.[7,8] In Ref. 7, an interior point-based solution for the two-dimensional conflict resolution problem was developed. These concepts for infinite time safety guarantees are extended in Ref. 8. Here, the optimal conflict-free trajectory is chosen as the one that minimizes a certain cost function. We also account for priorities among aircraft using the approach of Hu et al.[5] The protected zone around each aircraft is modeled as a cylinder. The disjunction involved when the protected zone is modeled is reformulated by the use of a continuous formulation. This approach obviates the need for simplifying assumptions such as level flight of aircraft or approximations of the protection zone. The resulting model is nonconvex and can pose difficulty when solutions are sought by the use of a nonlinear programming approach. To address this issue, we also present initialization strategies that enable fast and robust convergence of the optimal control problem. The approach can readily handle conflicts among multiple aircraft. We also present the effectiveness of our approach on a number of examples.

The key concept in the paper is a mathematical programming-based dynamic optimization framework for the accommodation of detailed dynamic aircraft models for the purposes of construction of optimal conflict-free trajectories for a given aircraft set. This presents a significant departure from the existing literature, which focuses predominantly on simple kinematic models. Note that conflict resolution algorithms that work with simple models may generate trajectories that are not necessarily flyable in practice. This issue of flyability of the optimal trajectories that are generated by any solution approach is critical to both safety and performance and necessitates the use of more realistic and detailed dynamic models. The framework presented in this paper addresses the flyability issue by allowance of the use of dynamic aircraft models at any desired level of detail. The dynamic optimization framework that involves an optimal control problem formulation, and its equivalent finite dimensional nonlinear program, is applicable irrespective of the actual model that is utilized. To place this presentation in context, we consider the examples presented in Ref. 5.

The paper is organized as follows: The following section describes a discretization procedure that recasts an optimal control problem, which is an infinite-dimensional dynamic optimization problem, into a finite-dimensional nonlinear program by the use of collocation on finite elements. This is followed by the description of nonlinear point-mass model of the aircraft and the initialization strategy for the same. Section IV briefly presents results for different scenarios. Finally, we conclude with directions for future work.

II. Formulation and Solution of Dynamic Optimization Problem

In this section, we describe a discretization procedure to convert an infinite-dimensional optimal control problem into a finite-dimensional nonlinear program. We also briefly describe the interior-point algorithm used to solve the resulting nonlinear program. More details on the algorithm can be found in Refs. 9 and 10.

A. Collocation on Finite Elements

A general form of the optimal control problem that applies to conflict resolution among multiple aircraft is as follows. Note that such a form accommodates any desired level of dynamic modeling detail; this is an important issue with respect to trajectory flyability:

$$\min_{\{w_1^{\mathrm{d}}, w_1^{\mathrm{a}}, u_1, \ldots, w_N^{\mathrm{d}}, w_N^{\mathrm{a}}, u_N\}} \sum_{n=1}^{N} \nu_n J_n\left(w_n^{\mathrm{d}}, w_n^{\mathrm{a}}, u_n\right)$$

$$\text{subject to} \quad \frac{\mathrm{d}w_n^{\mathrm{d}}}{\mathrm{d}t} = f\left(w_n^{\mathrm{d}}, w_n^{\mathrm{a}}, u_n\right); \; w_n^{\mathrm{d}}(t_0) = w_{n,0}^{\mathrm{d}}; \; w_n^{\mathrm{d}}(t_f) = w_{n,f}^{\mathrm{d}} \qquad \forall \quad n = 1, \ldots, N$$

$$g_{\mathrm{eq}}\left[w_n^{\mathrm{d}}(t), w_n^{\mathrm{a}}(t), u_n(t)\right] = 0, \qquad \forall \quad n = 1, \ldots, N$$

$$g_{\mathrm{ineq}}\left[w_{n_1}^{\mathrm{d}}(t), w_{n_1}^{\mathrm{a}}(t), u_{n_1}(t), w_{n_2}^{\mathrm{d}}(t), w_{n_2}^{\mathrm{a}}(t), u_{n_2}(t)\right] \geq 0 \qquad \forall \quad 1 \leq n_1 < n_2 \leq N$$

$$w_n^{\mathrm{d},L} \leq w_n^{\mathrm{d}}(t) \leq w_n^{\mathrm{d},U}, \qquad \forall \quad n = 1, \ldots, N$$

$$w_n^{\mathrm{a},L} \leq w_n^{\mathrm{a}}(t) \leq w_n^{\mathrm{a},U}, \qquad \forall \quad n = 1, \ldots, N$$

$$u_n^L \leq u_n(t) \leq u_n^U, \qquad \forall \quad n = 1, \ldots, N \tag{1}$$

where N is the number of aircraft involved, w_n^{d}, w_n^{a}, and u_n represent the differential, algebraic, and control variables of the individual aircraft in that order, g_{eq} are the algebraic equalities, and g_{ineq} are separation constraints between different pairs of aircraft. In general, the optimal control problem (1) cannot be solved analytically. Numerical approximations are used to convert the infinite-dimensional problem to a finite-dimensional problem. There are essentially two approaches to solve such dynamic optimization problems. The sequential approach solves the optimal control problem in the space of controls alone after the state variables are integrated in time. The inequalities that involve the differential and algebraic variables are appended to the objective function as a penalty term. In contrast, the simultaneous method solves the finite-dimensional problem in the space of differential, algebraic, and control variables. The approach also leads to a straightforward handling of the inequalities and bounds involving differential and algebraic variables. Though the resulting nonlinear program for the simultaneous method has more constraints and variables, it possesses specific sparsity patterns depending on the discretization scheme used. The sparse structure can be exploited to devise efficient decomposition schemes.

We will employ collocation on finite elements to discretize the optimal control problem (1). The profiles of the variables are approximated by a family of polynomials on finite elements. The time interval of interest $[t_0, t_f]$ is divided into ne finite elements of length h_i such that

$$\sum_{i=1}^{ne} h_i = t_f - t_0$$

Furthermore, we may define the time at the end of the intervals as

$$t_i := t_0 + \sum_{l=1}^{i} h_l, \qquad \forall \quad i = 1, \ldots, ne (t_{ne} = t_f)$$

We employ a monomial basis representation[11] for the differential and algebraic variables. The time profiles of differential and algebraic variables are approximated by the use of, respectively, the

derivatives and values evaluated at *ncol* collocation points within each element whose relative location is the same. The time points within the elements are defined as

$$t_{i,q} := t_{i-1} + h_i \rho_q, \qquad \forall \quad q = 1, \ldots, ncol$$

where $\rho_q \in [0, 1]$ are usually chosen to be the shifted roots of orthogonal polynomials of degree *ncol*. In this work, we use Radau points for ρ_q because they allow us to set constraints easily at the end of each element and stabilize the system when high index constraints are present. In addition, the monomial representation leads to smaller condition numbers and rounding errors.[11] A monomial basis representation[11] is used for the differential profiles as

$$w_n^{\mathrm{d}}(t) = w_{n,i-1}^{\mathrm{d}} + h_i \sum_{q=1}^{ncol} \Omega_q\left(\frac{t - t_{i-1}}{h_i}\right)\left(\frac{\mathrm{d}w_n^{\mathrm{d}}}{\mathrm{d}t}\right)_{i,q}$$

$$t \in [t_{i-1}, t_i], \qquad n = 1, \ldots, N \quad (2)$$

where $w_{n,i-1}^{\mathrm{d}}$ approximates the value of the differentiable variable at the beginning of element i, $w_n^{\mathrm{d}}(t_{i-1})$ and $(\mathrm{d}w_n^{\mathrm{d}}/\mathrm{d}t)_{i,q}$ approximates the first derivative of $w_n^{\mathrm{d}}(t)$ at time $t_{i,q}$. The polynomial Ω_q is of order *ncol*, satisfying

$$\Omega_q(0) = 0, \qquad q = 1, \ldots, ncol$$

$$\frac{\mathrm{d}\Omega_q}{\mathrm{d}t}(\rho_r) = \delta_{q,r}, \qquad q = 1, \ldots, ncol \qquad r = 1, \ldots, ncol$$

where ρ_r is the rth collocation point within each element. The control and algebraic profiles are approximated within each element i by the use of the monomial basis representation as

$$w_n^{\mathrm{a}}(t) = \sum_{q=1}^{ncol} \psi_q\left(\frac{t - t_{i-1}}{h_i}\right) w_{n,i,q}^{\mathrm{a}}, \qquad t_{i-1} < t \le t_i \quad (3)$$

$$u_n(t) = \sum_{q=1}^{ncol} \psi_q\left(\frac{t - t_{i-1}}{h_i}\right) u_{n,i,q}, \qquad t_{i-1} < t \le t_i \quad (4)$$

where $w_{n,i,q}^{\mathrm{a}}$ and $u_{n,i,q}$ represent the values of the algebraic and control variables, respectively, in each element i at collocation point q and ψ_q is a Lagrange polynomial of order *n*col satisfying

$$\psi_q(\rho_r) = \delta_{q,r}$$

The collocation formulation imposes continuity across the time elements for the differential variables (2) as

$$w_{n,i}^{\mathrm{d}}(t_i) = w_{n,i+1}^{\mathrm{d}}(t_i), \qquad \forall \quad i = 1, \ldots, ne - 1$$

whereas the algebraic and control variables are allowed to have discontinuities at the boundaries of the elements.

We assume that the number of finite elements *ne* and their lengths are predetermined. With this assumption, the substitution of the profile approximations and slacks for the inequality constraints yields the following nonlinear programming problem (NLP):

$$\min_{w \in \mathbb{R}^{n_w}} \phi(\boldsymbol{w}), \qquad \text{subject to} \quad c(\boldsymbol{w}) = 0, \qquad \boldsymbol{w}^L \le \boldsymbol{w} \le \boldsymbol{w}^U \quad (5)$$

where

$$\boldsymbol{w} = \left[\left(\frac{\mathrm{d}w_n^{\mathrm{d}}}{\mathrm{d}t}\right)_{i,q}, w_{n,i}^{\mathrm{d}}, w_{n,i,q}^{\mathrm{a}}, u_{n,i,q}\right]$$

$$\phi : \mathbb{R}^{n_w} \to \mathbb{R}, \qquad c : \mathbb{R}^{n_w} \to \mathbb{R}^{n_c}$$

We employ a barrier algorithm to solve the NLP. Optimal solutions for joint maneuvers typically bring aircraft to within the minimum separation. Different separation constraints are active, depending on which pair of aircraft are at the minimum separation. Given the large number of separation constraints $N(N-1)(ne)(ncol)/2$, an active set algorithm can be expensive if a good guess for the optimal active set is not readily available. Barrier algorithms[9,10] have been shown to overcome the combinatorial bottleneck of current sequential quadratic programming (SQP) methods of identifying the active inequality constraints. Encouraging results have been obtained on a number of process engineering problems with a large number of inequality constraints.[12]

B. NLP Algorithm

The NLP (5) is solved by the use of IPOPT,[10] an interior point algorithm. The algorithm follows a barrier approach, where the bounds on the variables $\boldsymbol{w}$ are replaced by a logarithmic barrier term that is added to the objective to yield, for problem (P_ν),

$$\min_w \varphi_\nu := \phi(\boldsymbol{w}) - \nu \sum_{j=1}^{n_w} \ell n\left(\boldsymbol{w}^{(j)} - \boldsymbol{w}^{L(j)}\right) - \nu \sum_{j=1}^{n_w} \ell n\left(\boldsymbol{w}^{U(j)} - \boldsymbol{w}^{(j)}\right)$$

subject to $c(\boldsymbol{w}) = 0$ with a barrier parameter $\nu > 0$. Here, $\boldsymbol{w}^{(j)}$ denotes the jth component of the vector $\boldsymbol{w}$. The barrier algorithm attempts to solve the NLP (5) by solving a sequence of barrier problems $\{P_{\nu_l}\}$ with decreasing barrier parameter, $\{\nu_l\} \to 0$. For a given barrier parameter $\nu > 0$, the logarithmic term in the objective function of barrier problem (P_ν) serves to push the iterates into the strict interior of the region defined by the bounds. As the barrier parameter ν is driven to zero, the influence of the logarithmic term is diminished and, under certain assumptions,[13] we are also able to recover solutions that make a bound active. In essence, the barrier algorithm approaches the solution to the barrier problem from the interior of the feasible region.

The interior point approach avoids having to identify the active inequalities at the solution and the combinatorial difficulty associated with it. The algorithm, IPOPT[10] solves for the stationary conditions of problem (P_ν). The stationary conditions of (P_ν) are

$$\nabla_w \phi(\boldsymbol{w}) + \nabla_w c(\boldsymbol{w}) \lambda_c - \nu(\boldsymbol{W} - \boldsymbol{W}^L)^{-1} \boldsymbol{e}_w + \nu(\boldsymbol{W}^U - \boldsymbol{W})^{-1} e_w = 0$$

$$c(\boldsymbol{w}) = 0 \quad (6)$$

where $\boldsymbol{W}$ denotes a diagonal matrix with the elements of vector $\boldsymbol{w}$ on the diagonal, $\boldsymbol{e}_w = [1 \;\; 1 \ldots 1 \;\; 1]^T$ is a vector of length n_w, and $\lambda_c \in \mathbb{R}^{n_c}$ is the Lagrange multiplier corresponding to the equality constraints. The preceding formulation is called primal because it involves only the variables $\boldsymbol{w}$ and not the multipliers corresponding to the bounds on $\boldsymbol{w}$. Instead, we can repose the preceding in primal–dual form by the introduction of variables λ^L and λ^U that converge to the multipliers for the bound constraints as $\nu \to 0$, under certain assumptions.[10,14] The primal–dual formulation is also known to lead to better conditioned linear systems than the primal formulation.[15] The primal–dual formulation is

$$\nabla_w \phi(\boldsymbol{w}) + \nabla_w c(\boldsymbol{w}) \lambda_c - \boldsymbol{\lambda}^L + \boldsymbol{\lambda}^U = 0, \qquad c(\boldsymbol{w}) = 0$$

$$(\boldsymbol{W} - \boldsymbol{W}^L)\boldsymbol{\lambda}^L = \nu \boldsymbol{e}_w, \qquad (\boldsymbol{W}^U - \boldsymbol{W})\boldsymbol{\lambda}^U = \nu \boldsymbol{e}_w \quad (7)$$

where λ^L and $\lambda^U \in \mathbb{R}^{n_w}$ are Lagrange multipliers corresponding, respectively, to the lower and upper bounds. The solution to the stationary conditions (7) is obtained by the application of Newton's method to the preceding system of equations. Given an iterate $(\boldsymbol{w}, \lambda_c, \lambda^L, \lambda^U)$, we obtain a candidate step by solving the following system of equations:

$$\begin{bmatrix} H(\boldsymbol{w}) & \nabla_w c(\boldsymbol{w}) & -I & I \\ \nabla_w c(\boldsymbol{w})^T & 0 & 0 & 0 \\ \Lambda^L & 0 & (\boldsymbol{W} - \boldsymbol{W}^L) & 0 \\ \Lambda^U & 0 & 0 & (\boldsymbol{W}^U - \boldsymbol{W}) \end{bmatrix} \begin{pmatrix} \triangle \boldsymbol{w} \\ \triangle \lambda_c \\ \triangle \lambda^L \\ \triangle \lambda^U \end{pmatrix}$$

$$= -\begin{bmatrix} \nabla_w \phi + \nabla_w c(\boldsymbol{w}) \lambda_c - \boldsymbol{\lambda}^L + \boldsymbol{\lambda}^U \\ c(\boldsymbol{w}) \\ (\boldsymbol{W} - \boldsymbol{W}^L)\boldsymbol{\lambda}^L - \nu \boldsymbol{e}_w \\ (\boldsymbol{W}^U - \boldsymbol{W})\boldsymbol{\lambda}^U - \nu \boldsymbol{e}_w \end{bmatrix} \quad (8)$$

where

$$H(\boldsymbol{w}) := \nabla_{ww}\phi(\boldsymbol{w}) + \sum_{i=1}^{n_c} \lambda_c^{(i)} \nabla_{ww} c^{(i)}(\boldsymbol{w})$$

I is the $n_w \times n_w$ identity matrix, and Λ^L, Λ^U, are $n_w \times n_w$ diagonal matrices with elements of vectors $\boldsymbol{\lambda}^L$, $\boldsymbol{\lambda}^U$, respectively, on the diagonal. The algorithm then calculates the next iterate $(\boldsymbol{w}^+, \lambda_c^+, \lambda^{L,+}, \lambda^{U,+})$ as follows:

$$\left(\boldsymbol{w}^+, \lambda_c^+, \lambda^{L,+}, \lambda^{U,+}\right) = \left(\boldsymbol{w}, \lambda_c, \lambda^L, \lambda^U\right) + \alpha\left(\triangle\boldsymbol{w}, \triangle\lambda_c, \triangle\lambda^L, \triangle\lambda^U\right) \tag{9}$$

where $\alpha \in (0, 1]$ is the fraction of the step to be taken. The fraction of the step is calculated to stay strictly within the bounds on $\boldsymbol{w}$, $\boldsymbol{\lambda}^L$, and $\boldsymbol{\lambda}^U$ and also to guarantee sufficient progress toward the solution of problem (P_v) as measured by the filter line search; this is a novel mechanism to promote convergence from poor initial points. The interested reader is referred to the work of Wächter and Biegler[14] and Wächter[10] for details on the convergence and implementation. IPOPT has been developed for solving large-scale NLP problems and has also been interfaced to a modeling language, AMPL.[16]

III. Aircraft Dynamics: Three-Degree-of-Freedom Model

In this section, we describe the three-dimensional conflict resolution of multiple aircraft by the use of NLP strategies. The formulation we propose in this section takes into account the point-mass aircraft dynamics. The model is a practical representation of the aircraft dynamics. The model is as shown here:

$$\frac{\mathrm{d}x_n}{\mathrm{d}t} = V_n \cos\gamma_n \cos\chi_n, \qquad x_n(t_0) = x_{n,0}, \quad x_n(t_f) = x_{n,f} \tag{10a}$$

$$\frac{\mathrm{d}y_n}{\mathrm{d}t} = V_n \cos\gamma_n \sin\chi_n, \qquad y_n(t_0) = y_{n,0}, \quad y_n(t_f) = y_{n,f} \tag{10b}$$

$$\frac{\mathrm{d}z_n}{\mathrm{d}t} = V_n \sin\gamma_n, \qquad z_n(t_0) = z_{n,0}, \quad z_n(t_f) = z_{n,f} \tag{10c}$$

$$\frac{\mathrm{d}V_n}{\mathrm{d}t} = \frac{T_n - D_n}{m_n} - g\sin\gamma_n, \qquad V_n(t_0) = V_{n,0} \tag{10d}$$

$$\frac{\mathrm{d}\gamma_n}{\mathrm{d}t} = \frac{g}{V_n}\left(\frac{L_n\cos\mu_n}{gm_n} - \cos\gamma_n\right), \qquad \gamma_n(t_0) = \gamma_{n,0} \tag{10e}$$

$$\frac{\mathrm{d}\chi_n}{\mathrm{d}t} = \frac{L_n\sin\mu_n}{m_n V_n\cos\gamma_n}, \qquad \chi_n(t_0) = \chi_{n,0} \tag{10f}$$

$$|z_n(t) - z_l(t)| \geq H \vee [x_n(t) - x_l(t)]^2 + [y_n(t) - y_l(t)]^2 \geq R^2$$
$$1 \leq n < l \leq N \tag{10g}$$

$$D_n(t) = 0.01\rho_{\mathrm{air}}[V_n(t)]^2 S_n + \frac{0.6[L_n(t)]^2}{\rho_{\mathrm{air}}[V_n(t)]^2 S_n} \tag{10h}$$

$$V_{n,\min} \leq V_n(t) \leq V_{n,\max}, \qquad |\mu_n(t)| \leq \mu_{n,\max}, \qquad |\gamma_n| \leq \gamma_{n,\max} \tag{10i}$$

$$0 \leq T_n(t) \leq T_{n,\max}, \qquad 0 \leq L_n(t) \leq L_{n,\max} \tag{10j}$$

where n indexes the aircraft, $(x_{n,0}, y_{n,0}, z_{n,0})$ and $(x_{n,f}, y_{n,f}, z_{n,f})$ denote the initial and final positions of aircraft n, respectively, V_n represents the ground speed of aircraft n, γ_n is the flight-path angle, χ_n is the heading angle, T_n is the engine thrust, D_n is the drag, L_n is the lift, m_n is the aircraft mass, μ_n is the bank angle, S_n is the wing area of the aircraft, and g is the acceleration due to gravity. The average density of air is ρ_{air}. Alternatively, the air density seen by each aircraft could be considered as a function of the altitude of aircraft $z_n(t)$. For the purpose of this paper, we will assume the air density to be constant.

The objective function considered in this model penalizes the change in speed in three directions, as well as changes in heading and flight-path angle. The optimal control problem can then be stated as

$$\min \frac{1}{2}\sum_{n=1}^{N} \nu_n \int_{t_0}^{t_f} \left[\left(\frac{\mathrm{d}x_n}{\mathrm{d}t}\right)^2 + \left(\frac{\mathrm{d}y_n}{\mathrm{d}t}\right)^2 + \eta^2\left(\frac{\mathrm{d}z_n}{\mathrm{d}t}\right)^2 + K_{\gamma,n}^2\left(\frac{\mathrm{d}\gamma_n}{\mathrm{d}t}\right)^2 + K_{\chi,n}^2\left(\frac{\mathrm{d}\chi_n}{\mathrm{d}t}\right)^2\right]\mathrm{d}t \tag{11}$$

subject to Eqs. (10a–10j), where η penalizes vertical maneuvers and $K_{\gamma,n}$ and $K_{\chi,n}$ are penalties for changes in the flight-path angle and heading angle. The weights ν_n are employed to prioritize the aircraft and specify the differences in maneuverability among the aircraft. The objective function shown here is an extension of the one proposed by Hu et al.,[5] and the states in the preceding model are aircraft position (x_n, y_n, z_n), ground speed V_n, flight-path angle γ_n, and heading angle χ_n. The degrees of freedom in the model are thrust T_n, lift L_n, and the bank angle μ_n. Formulation (11) is fairly general and more realistic with detailed dynamics, and it includes constraints and objectives that cannot be incorporated in earlier approaches.[5] Other path constraints and terminal constraints on flight-path angle and heading angle can be easily handled.

We propose to solve the optimal control problem by converting it to a finite-dimensional NLP. The problem is recast as an NLP by discretization it as shown in Sec. II.A. The key challenge in modeling the problem (11) is the disjunctive equation (10g) representing the protection zone around each aircraft. The disjunctive equation can be formulated by the use of continuous variables as described hereafter. Suppose, for simplicity that the disjunctive equation is given as

$$g_1(t) \geq 0 \vee g_2(t) \geq 0 \tag{12}$$

Equation (12) can be posed with continuous variables, as follows:

$$\lambda_1(t)g_1(t) + \lambda_2(t)g_2(t) \geq 0, \qquad \lambda_1(t) + \lambda_2(t) = 1$$
$$\lambda_1(t), \lambda_2(t) \geq 0 \tag{13}$$

The second equation in formulation (13) is critical to show equivalence to the disjunction (12). The equation denotes a normalization constraint for λ_1 and λ_2. Of course, the right-hand side could be any positive constant. In its absence, $g_1(\hat{t}) < 0$, $g_2(\hat{t}) < 0$, $\lambda_1(\hat{t}) = \lambda_2(\hat{t}) = 0$ for some $\hat{t}$ will satisfy the continuous formulation, but violate the disjunction. Nevertheless, the first equation in formulation (13) is nonconvex and can induce local minima. Another aspect of the formulation is that there can be a number of choices for $\lambda_1(t)$ and $\lambda_2(t)$ for a given $g_1(t)$ and $g_2(t)$ at any time instant. For example, if at time $t = t_0$, $g_1(t_0) > 0$ and $g_2(t_0) < 0$, then any choice of $[\lambda_1(t_0), \lambda_2(t_0)]$ from the set

$$\left\{(\lambda_1, \lambda_2) \;\middle|\; \begin{matrix} \dfrac{-g_2(t_0)}{g_1(t_0) - g_2(t_0)} \leq \lambda_1 \leq 1 \\ \lambda_2 = 1 - \lambda_1 \end{matrix}\right\} \tag{14}$$

satisfies the separation requirement (13) for the time instant t_0. This nonuniqueness of (λ_1, λ_2) can induce singularity in the Hessian of the Lagrangian of the discretized optimal control problem (5), resulting in poor asymptotic convergence rates. For this purpose, we append the objective function in the optimal control problem (11) with quadratic terms involving λ as

$$\int_{t_0}^{t_f} \left[\lambda_1(t)^2 + \lambda_2(t)^2\right]\mathrm{d}t \tag{15}$$

The additional terms in Eq. (15) help to pin down the solution from set (14) when the integral and the separation constraints are

discretized as

$$\lambda_1(t_0) = \begin{cases} \dfrac{-g_2(t_0)}{g_1(t_0) - g_2(t_0)}, & \text{if} \quad \dfrac{-g_2(t_0)}{g_1(t_0) - g_2(t_0)} \geq \dfrac{1}{2} \\ \dfrac{1}{2}, & \text{otherwise} \end{cases} \tag{16}$$

$$\lambda_2(t_0) = 1 - \lambda_1(t_0)$$

for the instance of $g_1(t_0) > 0$, and $g_2(t_0) < 0$. We can derive similar results for other realizations of the sign on $g_1(t_0)$ and $g_2(t_0)$. With this formulation, for the separation requirements and the additional objective terms, we can reformulate the optimal control problem (11) as follows: minimize

$$\frac{1}{2}\sum_{n=1}^{N} \nu_n \int_{t_0}^{t_f} \left[\left(\frac{\mathrm{d}x_n}{\mathrm{d}t}\right)^2 + \left(\frac{\mathrm{d}y_n}{\mathrm{d}t}\right)^2 + \eta^2 \left(\frac{\mathrm{d}z_n}{\mathrm{d}t}\right)^2 + K_{\gamma,n}^2 \left(\frac{\mathrm{d}\gamma_n}{\mathrm{d}t}\right)^2 + K_{\chi,n}^2 \left(\frac{\mathrm{d}\chi_n}{\mathrm{d}t}\right)^2 \right] \mathrm{d}t + \frac{1}{2}\sum_{n=1}^{N-1}\sum_{l=n+1}^{N} \int_{t_0}^{t_f} \left[\lambda_{n,l,1}(t)^2 + \lambda_{n,l,2}^2\right] \mathrm{d}t \tag{17}$$

subject to formulation (10a–10f, 10h–10j).

$$\left.\begin{aligned} &\lambda_{n,l,1}(t)\left\{[x_n(t) - x_l(t)]^2 + [y_n(t) - y_l(t)]^2 - R^2\right\} \\ &+ \lambda_{n,l,2}(t)\left\{[z_n(t) - z_l(t)]^2 - H^2\right\} \geq 0 \\ &\lambda_{n,l,1}(t) + \lambda_{n,l,2}(t) = 1 \\ &\lambda_{n,l,1}(t), \lambda_{n,l,2}(t) \geq 0 \end{aligned}\right\} \; 1 \leq n < l \leq N$$

where $\lambda_{n,l,1}$ and $\lambda_{n,l,2}$ play the role of λ_1 and λ_2 for the disjunctive separation constraints for each pair of aircraft (n, l), such that $1 \leq n < l \leq N$. By the use of the preceding formulation, we can now discretize the optimal control problem to obtain a finite-dimensional NLP as described in Sec. II.A.

A. Initializing the NLP

The NLP obtained from discretization of the optimal control problem (11) has general equality and inequality constraints. The NLP is solved with IPOPT.[10] Section II.B. describes, in brief, the IPOPT algorithm. The fast convergence of NLP algorithms to a solution can be guaranteed only from points sufficiently close to the solution. Because of this, all NLP algorithms employ globalization strategies to promote convergence from points far removed from the neighborhood of a solution. IPOPT, for instance, employs a filter to handle poor starting points. A number of researchers show that these strategies aid convergence and prove theoretical results under mild regularity assumptions. Despite this, there are a host of other factors such as ill conditioning and round-off error that greatly affect performance of the algorithms. Hence, for most real-time applications, it is imperative that the user provide a good initial guess to aid fast convergence of the algorithm to the solution. In the context of time-critical applications such as aircraft conflict resolution, the importance of good initialization increases manifold. We propose to utilize the approach by Hu et al.,[5] described hereafter, to initialize the problem.

Hu et al.[5] consider conflict resolution of aircraft with dynamics described by a simple kinematic model. The model is

$$\frac{\mathrm{d}x}{\mathrm{d}t} = v_x(t), \qquad \frac{\mathrm{d}y}{\mathrm{d}t} = v_y(t), \qquad \frac{\mathrm{d}z}{\mathrm{d}t} = v_z(t) \tag{18}$$

where x, y, and z represent the position of the aircraft along the different axes. The velocities of the aircraft in the x, y, and z directions at time t are, respectively, $v_x(t)$, $v_y(t)$, and $v_z(t)$. The maneuvers available for the aircraft to avoid conflict are changes in these velocities. Hu et al.[5] obtain conflict-free trajectories for aircraft described by the dynamics (18) using geometric techniques. The optimal conflict-free trajectories are obtained as a result of minimization of the following objective:

$$J(v_x, v_y, v_z) = \frac{1}{2}\int_{t_0}^{t_f} \left\{[v_x(t)]^2 + [v_y(t)]^2 + \eta^2[v_z(t)]^2\right\} \mathrm{d}t \tag{19}$$

where $\eta \geq 1$ is a coefficient introduced to penalize vertical maneuvers. The objective function (19) represents the amount of fuel required for the maneuver and accounts for the difference in vertical maneuverability of the aircraft. Note that if we neglect the penalties in changing the flight-path and heading angles, the objective function in the detailed model (11) reduces to the preceding objective. The conflict resolution among n aircraft with cylindrical protection zones can be posed as the following optimal control problem, minimize

$$\sum_{n=1}^{N} \nu_n J_n(v_{x,n}, v_{y,n}, v_{z,n})$$

subject to

$$\begin{aligned} &\frac{\mathrm{d}x_n}{\mathrm{d}t} = v_{x,n}(t), \quad x_n(t_0) = x_{n,0}, \quad x_n(t_f) = x_{n,f} \quad n = 1, \ldots, N \\ &\frac{\mathrm{d}y_n}{\mathrm{d}t} = v_{y,n}(t), \quad y_n(t_0) = y_{n,0}, \quad y_n(t_f) = y_{n,f} \quad n = 1, \ldots, N \\ &\frac{\mathrm{d}z_n}{\mathrm{d}t} = v_{z,n}(t), \quad z_n(t_0) = z_{n,0}, \quad z_n(t_f) = z_{n,f} \quad n = 1, \ldots, N \\ &[x_n(t) - x_l(t)]^2 + [y_n(t) - y_l(t)]^2 \geq R^2 \vee |z_n(t) - z_l(t)| \geq H \quad 1 \leq n < l \leq N \end{aligned} \tag{20}$$

Hu et al.[5] are able to obtain considerable insight for the two-aircraft conflict resolution. They prove that solution of problem (20) is equivalent to finding the shortest path $(x_{n,0}, y_{n,0}, z_{n,0}) \rightarrow (x_{n,f}, y_{n,f}, z_{n,f})$, in suitably transformed coordinates, in the presence of a static cylindrical obstacle centered at the origin. Thus, the optimal control problem is now reduced to finding the shortest curve between two points in three dimensions that avoids an obstacle. Efficient numerical procedures that involve simple bound constrained minimization of a convex objective are proposed to calculate the solutions for different configurations of $(x_{n,0}, y_{n,0}, z_{n,0})$ and $(x_{n,f}, y_{n,f}, z_{n,f})$. The preceding procedure does not necessarily yield conflict-free trajectories in the multi-aircraft scenario. This is due to the potential domino effect, where conflict resolution between two aircraft might result in new conflicts. For this case, Hu et al. consider joint piecewise linear maneuvers parameterized by a waypoint for each aircraft. The optimal control problem then reduces to a finite-dimensional problem of location of the waypoints of each aircraft to minimize the objective function (19). The problem is convexified by the use of an inner approximation of the feasible region. Half-planes are generated that approximate the feasible region of the waypoints to resolve the conflict between pairs of aircraft. The resulting problem is a convex quadratic program for which well-developed solvers exist. The trajectories obtained in this manner are guaranteed to be conflict free, but there could be room for improvement because the feasible region is underestimated.

The solution obtained from the procedure of Hu et al.[5] can be utilized to obtain an initial guess for the NLP resulting from the discretization of the optimal control problem (11). The solution of Hu et al. involves only the position and velocities in the three directions. To obtain an initial guess, we employ the following strategy:

1) Solve the optimal control problem (20) by the use of the procedure of Hu et al.[5] to obtain the trajectories of each aircraft $(x_n^{\mathrm{Hu}}, y_n^{\mathrm{Hu}}, z_n^{\mathrm{Hu}})$.

2) Fix the trajectories of each aircraft in the three-degree-of-freedom model (10) to the solution $(x_n^{\mathrm{Hu}}, y_n^{\mathrm{Hu}}, z_n^{\mathrm{Hu}})$ obtained from Hu et al. procedure.

3) Solve the square system of equations (10a–10f) and (10h) to obtain ground speed, flight-path angle, heading angle, lift, thrust, and bank angle.

The preceding procedure yields a solution that satisfies the separation constraints (10g) as in Ref. (5). By the use of this as the initial guess, we may now solve the NLP resulting from the discretization of the optimal control problem (11). We have had success in obtaining an initial guess using the forgoing strategy for all of the scenarios we have considered. Note that problem (20) does not consider the effects of gravity or air drag, and it is not always flyable by the detailed model (10). For example, the bounds on some of the variables in the model (10i) and (10j) may be violated by the solution of problem (20). We have observed convergence on the initialization problem in all our runs, but the solution can violate the bounds. We may then perform a further refinement of the preceding solution at the expense of violating the separation constraints to obtain a solution that is flyable by the detailed model (10a–10f). This will also entail more computational effort and time. Instead, we modify the discretized NLP (5) based on the violated bounds. We relax the violated bounds by adding nonnegative artificial variables and penalize them in objective function. To explain the procedure, suppose that the solution of Hu et al. violates the lower bound on elements $\boldsymbol{w}_i$ of vector $\boldsymbol{w}$ for indices $i \in I^{\mathrm{lb}} \subseteq \{1, \ldots, n_w\}$ and the upper bound on elements $\boldsymbol{w}_i$ of vector $\boldsymbol{w}$ for indices $i \in I^{\mathrm{ub}} \subseteq \{1, \ldots, n_w\}$. We then reformulate the NLP, as follows: Minimize

$$f(\boldsymbol{w}) + \theta(s^L + s^U)$$

subject to

$$\begin{aligned} c(\boldsymbol{w}) &= 0 \\ \boldsymbol{w}^{L,(i)} - s^{L,(i)} &\le \boldsymbol{w}^{(i)}, \qquad \forall \quad i \in I^{\mathrm{lb}} \\ \boldsymbol{w}^{(i)} &\le \boldsymbol{w}^{U,(i)} + s^{U,(i)}, \qquad \forall \quad i \in I^{\mathrm{ub}} \\ \boldsymbol{w}^{L,(i)} &\le \boldsymbol{w}^{(i)}, \qquad \forall \quad i \in \{1, \ldots, n_w\} \setminus I^{\mathrm{lb}} \\ \boldsymbol{w}^{(i)} &\le \boldsymbol{w}^{U,(i)}, \qquad \forall \quad i \in \{1, \ldots, n_w\} \setminus I^{\mathrm{ub}} \\ s^L, s^U &\ge 0 \end{aligned} \tag{21}$$

where $s^L \in \mathbb{R}^{|I^{\mathrm{lb}}|}$ and $s^U \in \mathbb{R}^{|I^{\mathrm{ub}}|}$ are slacks for the violated constraints and $\theta > 0$ is a penalty for the violated constraints. With the preceding reformulation, the solution of Hu et al. is a feasible initial guess for a suitable choice of the artificial variables s. Furthermore, if the conflict cannot be resolved within the constraints of the problem instance, then the preceding formulation has the ability to terminate at a solution that satisfies dynamics with a measure of violation of bounds on the variables such as thrust, flight-path angle, etc. The preceding reformulation has proved very useful in the acceleration of convergence from an otherwise infeasible initialization for the original discretized formulation (5). This experience reiterates the value of a simplified model in its ability to provide insights to the original problem.

IV. Results

The section describes the results obtained from the use of our approach to generate conflict-free maneuvers for aircraft governed by nonlinear point mass models (10) by the use of scenarios from Hu et al.[5]

We now present results from the use of our approach to resolution of conflict scenarios when aircraft are modeled with detailed dynamics. In all scenarios, the aircraft are assumed to be heading to the final position along the straight line from their initial positions and z coordinate of position coordinates is the aircraft altitude in nautical miles. The values of the bounds on variables and initial values (10) for the aircraft are as follows: The mass of the aircraft m_n and wing reference area S_n are taken to be 1.87×10^5 lb and 2.52×10^3 ft^2, respectively. The bounds on the variables are $V_{n,\min} = 146$ kn, $V_{n,\max} = 467$ kn, $\mu_{n,\max} = \gamma_{n,\max} = 20$ deg, $T_{n,\max} = 0.2m_n$ lbf, and $L_{n,\max} = 2m_n$ lbf. An important feature of the aircraft model in Eq. (10) is that the value of 0.6 for the drag coefficient in Eq. (10h) is much larger than the nominal value, and, hence, the model corresponds to a hypothetical aircraft. The solution framework outlined in earlier sections, which is the focus of this paper, will continue to hold regardless of the model. The initial values for the state variables are obtained from those required for a constant-speed straight line motion from $(x_{n,0}, y_{n,0}, z_{n,0})$ to $(x_{n,f}, y_{n,f}, z_{n,f})$ in time $t_f - t_0$. The time for resolution of the conflict $(t_f - t_0)$ is 15 min in the two-aircraft cases and 20 min in the others. For all problems, we have used a discretization with $10(= ne)$ elements and $3(= ncol)$ collocation points. The solutions to the discretized problems all satisfy the stationary conditions to a tolerance of 10^{-6}. Hence, the reported solutions are locally optimal for the given discretization. The problem size, iteration, and CPU time requirements are in Table 1. The iteration number and CPU times for given number of aircraft are the average times required to solve the different scenarios discussed hereafter. The computations are performed on a 2.26-GHz Intel Pentium 4 processor running LINUX as the operating system.

Table 1 Problem size and CPU time required for cases of different aircraft (detailed model)

Number of aircraft	Number of variables	Number of constraints	Iterations	CPU time, s
2	1212	1008	15	0.3
4	2850	2289	70	8
8	7304	5619	386	651

The number of iterations, as well as the CPU time to obtain a solution, depends to a certain degree on the initial guess. All of the scenarios are initialized with the procedure described in the preceding section. In our experience, the more interesting conflict scenarios result in the solution from the Hu et al. algorithm, violating some of the bound constraints, usually the upper bound on thrust. For example, in the eight-aircraft case, all but two of the aircraft violate the upper bound on thrust. As a result, we require more iterations to converge to a solution. To gauge the effect on computing effort with increasing aircraft, we compare the time per iteration in each case. The time per iteration increases 5-fold from the 2-aircraft to the 4-aircraft case and 15-fold for the 8-aircraft case over the 4-aircraft cases. The computationally intensive part of each iteration is the factorization involved in the calculation of the search direction (8). To handle cases with increased time elements or aircraft, we will require efficient decomposition schemes for the solution of the resulting large-scale NLP.

In the following subsections, we present results from the use of our approach on various conflict resolution scenarios. In most of the conflict resolution scenarios that we considered, the trajectory of Hu et al. violated the bounds. For scenarios where this did not occur, the improvement in the objective over that of Hu et al. is minor, approximately 0.3–0.5%. Nevertheless, the significant feature of our algorithm is that we can generate flyable trajectories even when the initial solutions from Hu et al. algorithm do not. We describe a typical situation that will illustrate the value of our approach. Consider the resolution of the conflict between two aircraft with initial and final positions as aircraft 1 $(0, 40, 4) \rightarrow (80, 40, 4)$ and aircraft 2 $(40, 80, 4) \rightarrow (40, 0, 4)$. The protection zone has a radius $R = 5$ n mile and height $H = 2000$ ft. The values for penalties in the objective are $\eta = 5$, $K_{\gamma,n} = 5$, and $K_{\chi,n} = 5$, and the priority for each aircraft was 0.9 for the first and 0.1 for the other. In this example, and the others to follow, we have employed protection zones with larger than the prescribed 1000 ft for aircraft flying below altitudes of 29,000 ft. The yz projection of the trajectory of aircraft 2 obtained from algorithm of Hu et al. and our algorithm are provided in Fig. 1. Thrust obtained from each of the solutions and the upper

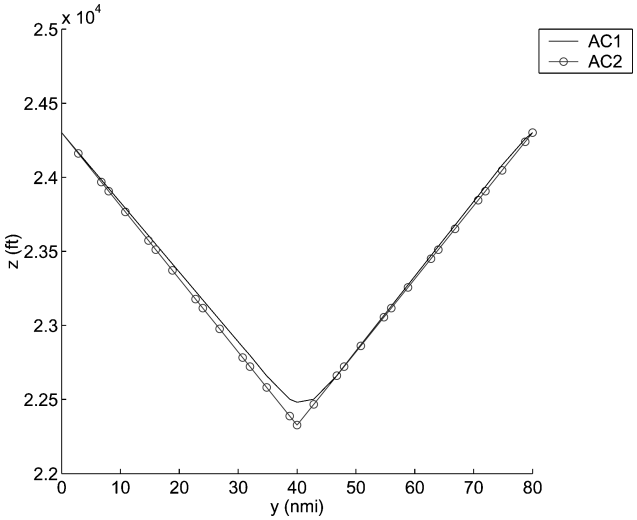

Fig. 1a Projection onto *yz* plane of aircraft maneuvers from our approach and that of Hu et al. for aircraft 2: $\eta = 5, K_{\gamma,n} = K_{\chi,n} = 5, \nu_1 = 0.9,$ and $\nu_2 = 0.1$.

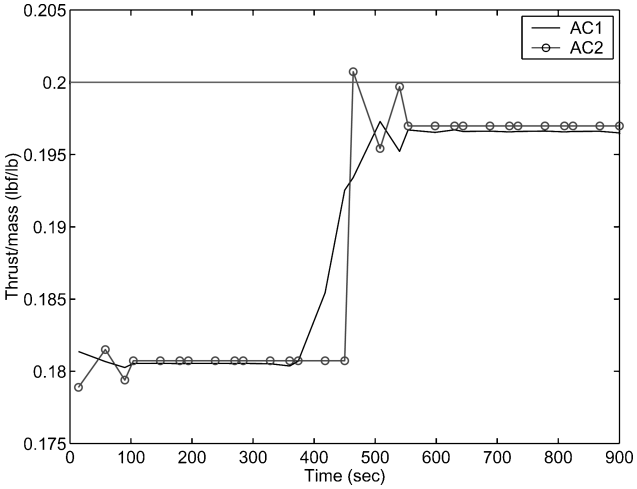

Fig. 1b Thrust profile for the solutions from our approach and that of Hu et al. for aircraft 2: $\eta = 5, K_{\gamma,n} = K_{\chi,n} = 5, \nu_1 = 0.9,$ and $\nu_2 = 0.1$.

bound on thrust (as a line with dashes and dots) are shown as well. It is clear from Fig. 1 that the solution of Hu et al. violates the bound on thrust due to the sharp maneuver at the waypoint. The solution from our approach smooths the turn of the aircraft at the waypoint and also results in a solution that does not violate the bound. Evidently, the approach we describe helps to obtain a solution that is not only flyable by the detailed dynamics but also satisfies the bound constraints.

A. Two-Aircraft Scenarios

The following summarizes the results of conflict resolution among two aircraft. The initial and final positions of the aircraft are as follows: aircraft 1 $(0, 40, 4) \rightarrow (80, 40, 4)$ and aircraft 2 $(40, 0, 4) \rightarrow (40, 80, 4)$. The values of ν_n, η, $K_{\gamma,n}$, and $K_{\chi,n}$ are given along with Fig. 2. The protection zone of aircraft has radius 5 n mile and height 2000 ft. Figure 2 are shown for varying weights ν_n. In Fig. 2b, aircraft 1 has greater priority than aircraft 2, and as a result, the second aircraft plays a greater role in ensuring that aircraft are conflict free. In both cases, the kinematic solution does not violate any bounds.

B. Four-Aircraft Scenarios

We consider the conflict resolution for aircraft with the following initial and final positions: aircraft 1 $(0, 100, 4) \rightarrow (100, 0, 4)$; aircraft 2 $(60, 0, 4) \rightarrow (40, 100, 4)$; aircraft 3 $(90, 90, 4) \rightarrow (0, 0, 4)$; and aircraft 4 $(100, 70, 4) \rightarrow (0, 40, 4)$. The radius of the protection zone of aircraft is increased to 10 n mile, and the height is 2000 ft. All aircraft have equal priority in the cases presented. In the first case, the vertical maneuver penalty η is 5, whereas it is 25 in the second. The kinematic solution violates the thrust bound in both cases. Aircraft 2–4 violate the thrust bound in the first case, whereas all aircraft violate thrust bound in the second case. The three-dimensional and top view plots in Figs. 3a and 4a are the aircraft trajectories for different values of maneuver penalties. It is clear from Figs. 3a and 4a that as the vertical penalty is increased, the aircraft avoid vertical maneuvers (Figs. 3 and 4). As a result, the aircraft remain conflict free using only horizontal maneuvers, namely, heading angle changes as seen in the projection of the trajectories onto the xy plane shown in Figs. 3 and 4.

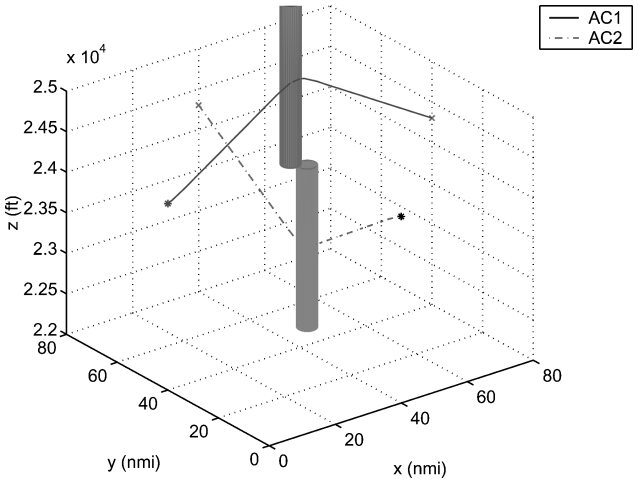

Fig. 2a Three-dimensional view of an optimal resolution maneuver for orthogonal two-aircraft encounter: $\eta = 5$, $K_{\gamma,n} = K_{\chi,n} = 5$, and $\nu_1 = \nu_2 = 0.5$.

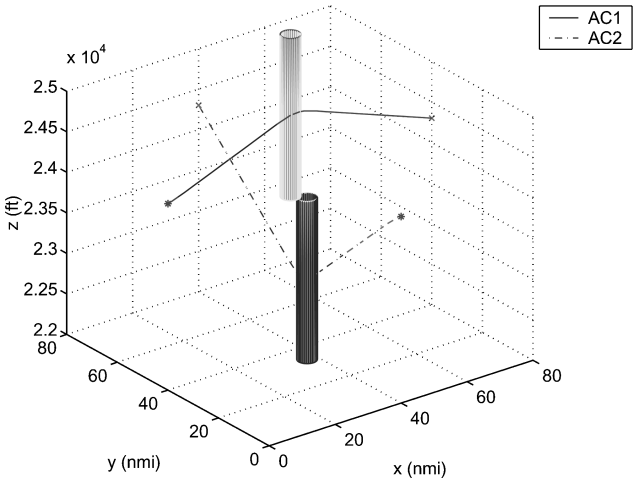

Fig. 2b Three-dimensional view of an optimal resolution maneuver for orthogonal two-aircraft encounter: $\eta = 5$, $K_{\gamma,n} = K_{\chi,n} = 5$, $\nu_1 = 0.7$, and $\nu_2 = 0.3$.

C. Eight-Aircraft Scenario

Finally, we have results from conflict resolution of the eight-aircraft encounter. The first four aircraft are the same as in the preceding subsection, and the initial and final positions of the remaining are aircraft 5, $(55, 90, 3.7) \rightarrow (50, 0, 3.7)$; aircraft 6, $(5, 10, 3.7) \rightarrow (50, 100, 3.7)$; aircraft 7, $(0, 55, 3.7) \rightarrow (90, 45, 4)$; and aircraft 8, $(10, 55, 3.7) \rightarrow (100, 45, 4)$. The radius of protection zones of aircraft are increased to 10 n mile and the height is 2000 ft. The kinematic solution violates the thrust bound for all but aircraft 1 and 3. Figure 5 shows the maneuver.

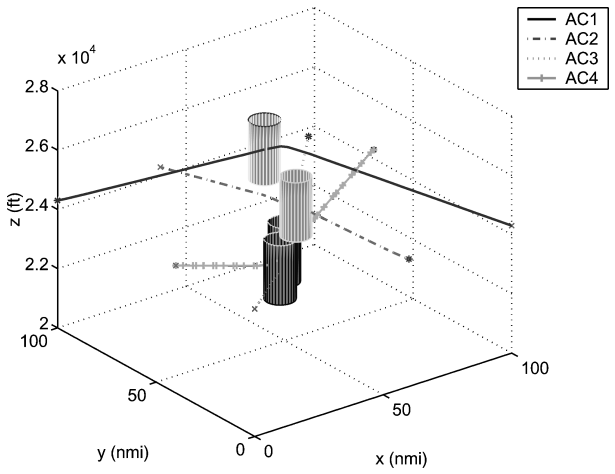

Fig. 3a Three-dimensional view of an optimal resolution maneuver for four-aircraft encounter: $\nu_n = 1/4$, $\eta = 5$, $K_{\gamma,n} = 5$, and $K_{\chi,n} = 5$.

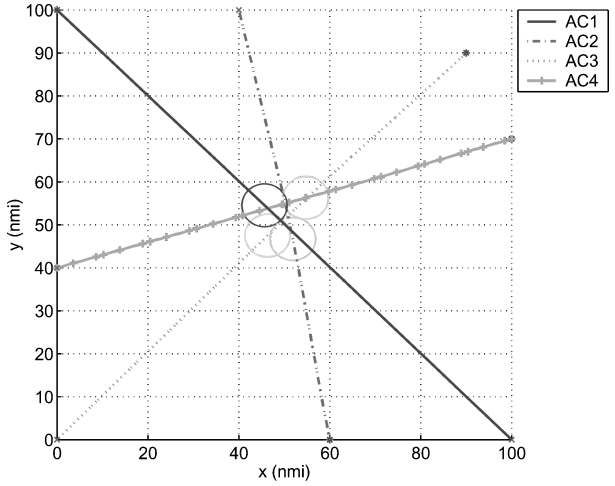

Fig. 3b Top view of an optimal resolution maneuver for four-aircraft encounter: $\nu_n = 1/4$, $\eta = 5$, $K_{\gamma,n} = 5$, and $K_{\chi,n} = 5$.

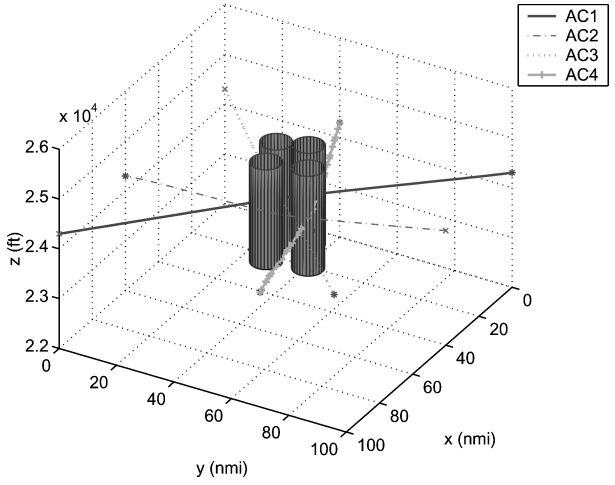

Fig. 4a Three-dimensional view of an optimal resolution maneuver for four-aircraft encounter: $\nu_n = 1/4$, $\eta = 25$, $K_{\gamma,n} = 5$, and $K_{\chi,n} = 5$.

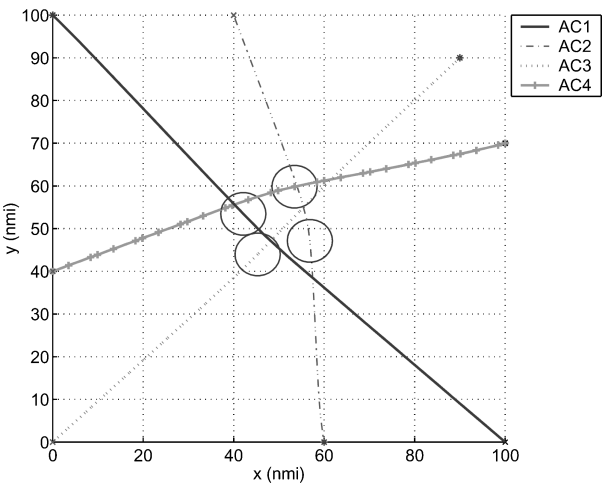

Fig. 4b Top view of an optimal resolution maneuver for four-aircraft encounter: $\nu_n = 1/4$, $\eta = 25$, $K_{\gamma,n} = 5$, and $K_{\chi,n} = 5$.

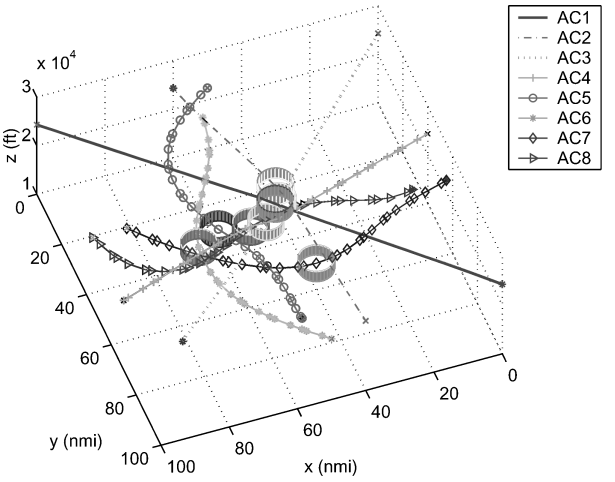

Fig. 5a Three-dimensional view of an optimal resolution maneuver for eight-aircraft encounter: $\nu_n = 1/8$, $\eta = 15$, $K_{\gamma,n} = 15$, and $K_{\chi,n} = 5$.

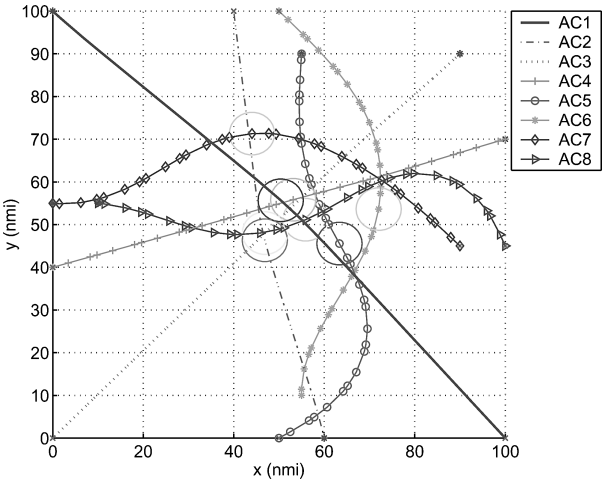

Fig. 5b Projection onto *xy* plane of an optimal resolution maneuver for eight-aircraft encounter: $\nu_n = 1/8$, $\eta = 15$, $K_{\gamma,n} = 15$, and $K_{\chi,n} = 5$.

D. Discussion

The performance of our approach when detailed dynamics of the aircraft are considered [model (11)] is very encouraging. The geometric approach of Hu et al. is not applicable in the context of detailed models, but we can obtain a reasonably good initialization for our NLP by the use of their solutions. Hu et al. also consider a more constrained model with bounds on the velocity and the angle between the two legs of their maneuver. However, lower bounds cannot be accommodated on velocity in their conic programming approach because these will be nonconvex constraints. Also, model (18) does not incorporate initial velocities, whereas detailed model (10) does. Quite conceivably, the initial velocities may differ substantially from the velocity in that leg. Hence, the initialization strategy for model (10) may yield a solution with dramatic velocity changes in the first few elements. Hu et al. also acknowledge this deficiency and suggest the inclusion of an initial buffer to

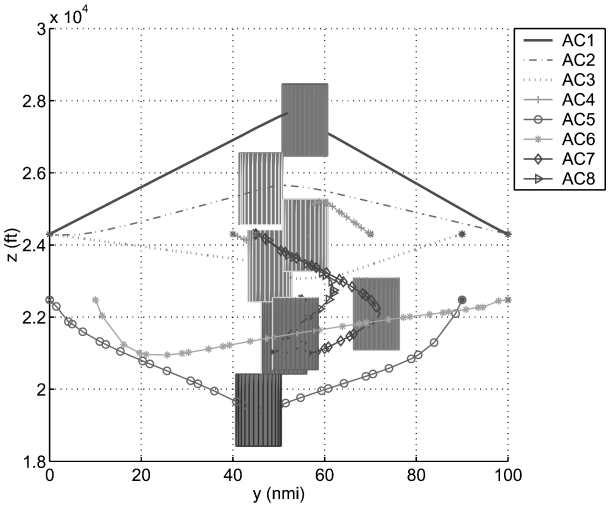

Fig. 5c Projections onto *yz* plane of an optimal resolution maneuver for eight-aircraft encounter: $\nu_n = 1/8$, $\eta = 15$, $K_{\gamma,n} = 15$, and $K_{\chi,n} = 5$.

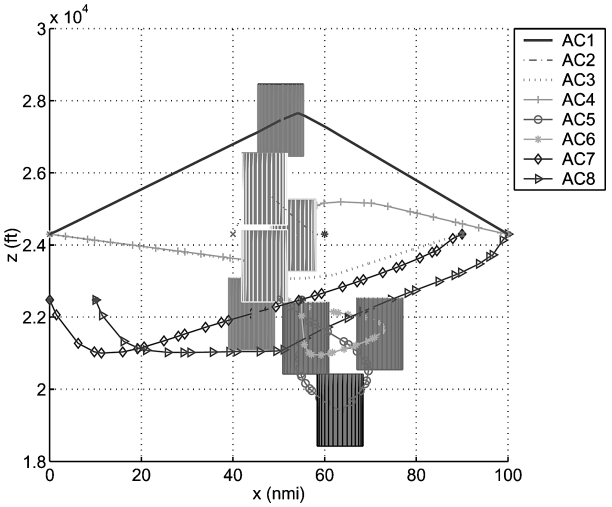

Fig. 5d Projections onto *xz* plane of an optimal resolution maneuver for eight-aircraft encounter: $\nu_n = 1/8$, $\eta = 15$, $K_{\gamma,n} = 15$, and $K_{\chi,n} = 5$.

accomplish the velocity changes that can render their solution suboptimal. Similarly, there might be sharp changes in velocity at the waypoints with similar effects. Clearly, the solution of the model of Hu et al., if flyable according to the detailed model, can be used as an initial guess for the NLP and improved on. Additional testing is then necessary to assess fully the strengths and weaknesses of our approach.

V. Conclusions

Three-dimensional coordinated maneuvers for resolution of conflicts are presented. The aircraft are described by nonlinear point-mass models with cylindrical protection zones. We have also included trajectory constraints to exclude unrealistic maneuvers. The optimal maneuvers are obtained as the solution of an optimal control problem that minimizes a cost function. We have also presented efficient initialization strategies that allow us to obtain solutions to the optimal control problem reliably. The computation times for most of the problems is relatively low. The initialization strategies require less than 1 min in all cases. We also propose strategies to handle infeasible initializations and infeasible problem instances. The computation time for the optimization problem ranged from about 1 min, for up to four aircraft scenarios, to about 11 min for the eight aircraft case when the nonlinear point mass model was used on a 2.26-GHz Intel Pentium 4 processor running LINUX as the operating system. The time per iteration increases significantly with the number of aircraft involved. The bulk of the time is spent in handling the linear algebra. The optimization problem involved has structure and lends itself to efficient decomposition schemes to reduce the computation times. The proposed framework can easily incorporate no-fly zones and can also handle high-fidelity models in a straightforward manner.

Acknowledgments

We acknowledge financial support from the Defense Advanced Research Projects Agency SEC Contract F33615-01-C-1848. We thank Jianghai Hu and Shankar Sastry for providing us with the MATLAB® implementation of their conflict resolution algorithm and also Michael Elgersma at Honeywell Laboratories Minneapolis, Minnesota, for insightful discussions pertaining to the detailed dynamic model used in this work.

References

[1]"Free Flight Implementation: Final Report of RTCA Task Force 3," RTCA, Washington, DC, Oct. 1995.

[2]Hwang, I., and Tomlin, C. J., "Protocol-Based Conflict Resolution for Air Traffic Control," Technical Rept., Dept. of Aeronautics and Astronautics, Stanford Univ., Stanford, CA, 2001.

[3]Zhao, Y., and Schultz, R., "Deterministic Resolution of Two Aircraft Conflict in Free Flight," AIAA Guidance, Navigation and Control Conf., 1997.

[4]Frazzoli, E., Mao, Z.-H., Oh, J.-H., and Feron, E., "Resolution of Conflicts Involving Many Aircraft via Semidefinite Programming, " *Journal of Guidance, Control, and Dynamics*, Vol. 24, No. 1, 2001, pp. 79–86.

[5]Hu, J., Pradini, M., and Sastry, S., "Three Dimensional Optimal Coordinated Maneuvers for Aircraft Conflict Avoidance," *Journal of Guidance, Control, and Dynamics*, Vol. 25, No. 5, 2002, pp. 888–900.

[6]Menon, P. K., Sweriduk, G. D., and Sridhar, B., "Optimal Strategies for Free-Flight Air Traffic Conflict Resolution," *Journal of Guidance, Control, and Dynamics*, Vol. 22, No. 2, 1999, pp. 202–211.

[7]Gopal, V., and Schulz, R., "2-D Multiaircraft Conflict Resolution with Interior Point Methods," *Sixth Society for Industrial and Applied Mathematics Conference on Optimization*, Society for Industrial and Applied Mathematics, Philadelphia, 1999.

[8]Oishi, M., Gopal, V., Tomlin, C., and Godbole, D., "Addressing Multi-objective Control: Safety and Performance Through Constrained Optimization," *Hybrid Systems: Computation and Control, Lecture Notes in Computer Science 2034*, Springer, New York, 2001, pp. 459–472.

[9]Biegler, L. T., Cervantes, A. M., and Wächter, A. W., "Advances in Simultaneous Strategies for Dynamic Process Optimization," *Chemical Engineering Science*, Vol. 57, No. 4, 2002, pp. 575–593.

[10]Wächter, A. W., and Biegler, L.T., "Global and Local Convergence of Line Search Filter Methods for Nonlinear Programming," Technical Rept., Dept. of Chemical Engineering, Carnegie Mellon Univ., Pittsburgh, PA, 2001.

[11]Bader, G., and Ascher, U., "A New Basis Implementation for Mixed Order Boundary Value ODE Solver," *SIAM Journal on Scientific and Statistical Computing*, Vol. 8, No. 4, 1987, p. 483.

[12]Cervantes, A. M., Wächter, A. W., Tütüncü, R. H., and Biegler. L. T., "A Reduced Space Interior Point Strategy for Optimization of Differential Algebraic Systems," *Computers and Chemical Engineering*, Vol. 24, No. 1, 2000, pp. 39–51.

[13]Fiacco, A. V., and McCormick, G. P., "Nonlinear Programming: Sequential Unconstrained Minimization Techniques," Wiley, New York, 1968.

[14]Wächter, A. W., "Interior Point Methods for Large-Scale Nonlinear Programming with Applications in Process Systems Engineering," Ph.D. Dissertation, Chemical Engineering Dept., Carnegie Mellon Univ., Pittsburgh, PA, 2002.

[15]Wright, M. H., "Ill-Conditioning and Computational Error in Interior Methods for Nonlinear Programming," *SIAM Journal on Optimization*, Vol. 9, No. 1, 1998, pp. 84–111.

[16]Fourer, R., Gay, D., and Kernighan, B., *AMPL*, Scientific Press, South San Francisco, CA, 1993.